Energy, Mines and Resources Canada
Énergie, Mines et Ressources Canada

CANMET

Canada Centre for Mineral and Energy Technology
Centre canadien de la technologie des minéraux et de l'énergie

Mining Research Laboratories
Laboratoires de recherche minière

PRELIMINARY RESULTS OF PILLAR-BACKFILL CONFINEMENT TESTS

B. Arjang

DIVISION REPORT MRL 91-063(TR) MARCH 1991

Canada

91-06271/

PRELIMINARY RESULTS OF PILLAR-BACKFILL CONFINEMENT TESTS

B. Arjang

DIVISION REPORT MRL 91-063(TR) MARCH 1991

This document is an internal client report prepared primarily for [illegible] and internal [illegible] purposes. It does not necessarily represent the views of the authors or the Canada Centre for Mineral and Energy Technology (CANMET)

Ce document est un rapport [illegible] préparé principalement [illegible] et interne [illegible] de CANMET)

36 pp

MICROMEDIA

PRELIMINARY RESULTS OF PILLAR-BACKFILL CONFINEMENT TESTS

B. Arjang*

ABSTRACT

A series of large scale experimental work was performed to demonstrate the interaction of pillar-backfill. The pillar-backfill specimens, using 136 mm diameter rock cores and cemented tailings of varying cement content, were confined in an aluminum cylinder. The complete load-deformation curves were recovered from simultaneous compression on composite pillar-backfill specimens in an 18 MN 'soft' testing machine. The preliminary data from this exploratory investigation indicate that violent pillar failure is controlled by backfill confinement and the failure mode and post-failure characteristics are primarily related to fill stiffness and the initial gap between the fill specimen and the loading platen.

Key words: Backfill; Pillar; Failure mode; Load-deformation.

*Research Scientist, Elliot Lake Laboratory, CANMET, Energy, Mines and Resources Canada, Elliot Lake, Ontario.

RÉSULTATS PRÉLIMINAIRES D'ESSAIS DE CONFINEMENT D'ÉCHANTILLONS DE PILIER-REMBLAI

B. Arjang*

RÉSUMÉ

Une série d'expériences à grande échelle ont été menées pour démontrer qu'il y a interaction pilier-remblai. Les échantillons de pilier-remblai, choisis à même des carottes de roche de 136 mm de diamètre et des résidus cimentés de teneur variable en ciment ont été confinés dans un cylindre d'aluminium. Les courbes charge-déformation complètes ont été établies par compression simultanée d'échantillons composites pilier-remblai dans une machine de sollicitation "douce" de 18 MN. Les données préliminaires de cette recherche exploratoire indiquent que la rupture violente des piliers est régie par le confinement des piliers, et que le mode de rupture et les caractéristiques après rupture sont principalement reliés à la rigidité du remblai et à l'écartement initial entre l'échantillon de remblai et la plaque de chargement.

Mots clés: remblai; pilier; mode de rupture; charge-déformation.

*Chercheur scientifique, Laboratoire d'Elliot Lake, CANMET, Énergie, Mines et Ressources Canada, Elliot Lake (Ontario).

CONTENTS

	Page
ABSTRACT	i
RESUME	ii
INTRODUCTION	1
ROCK-FILL SPECIMEN PREPARATION AND TESTING	1
PRELIMINARY RESULTS	3
DISCUSSION	4
ACKNOWLEDGEMENT	6
REFERENCES	6

TABLE

No.		
1.	Summary of confined pillar-backfill testing	7

FIGURES

1.	Sectional diagram of testing configuration	8
2.	Photographs showing the pillar-backfill test specimen in the aluminum cylinder	9
3.	Load-displacement curves from pillar-backfill confinement tests	10
4.	Load-displacement curves from post-failure compression on confined pillar-backfill specimens	11
5.	Relationship between vertical stress on the confined pillar-backfill and lateral stress in backfill	12
6.	Combined graphs of load-displacement and post-failure compression from pillar-backfill confinement; backfill ratio 10:1, test No. PBF-01, PBF-02 and PBF-03	13
7.	Combined graphs of load-displacement and post-failure compression from pillar-backfill confinement; backfill ratio 20:1, test No. PBF-04 and PBF-05	14
8.	Combined graphs of load-displacement and post-failure compression from pillar-backfill confinement; backfill ratio 30:1, test No. PBF-07 and PBF-11	15
9.	Combined graphs of load-displacement and post-failure compression from pillar-backfill confinement; backfill ratio 40:1, test No. PBF-09 and PBF-10	16
10.	Combined graphs of load-displacement and post-failure compression from pillar-backfill confinement; backfill ratio 50:1, test No. PBF-13 and PTG-12 pillar-tailings	17

11. Relationship between the residual strength and the backfill tailings:cement ratio 18

12. Load-displacement curves from uniaxial compression cycles on a confined backfill (30:1) 19

13. Pillar post-failure appearance, test PBF-01 20

14. Pillar post-failure appearance, test PBF-02 21

15. Pillar post-failure appearance, test PBF-03 22

16. Pillar post-failure appearance, test PBF-04 23

17. Pillar post-failure appearance, test PBF-05 24

18. Pillar post-failure appearance, test PBF-06 25

19. Pillar post-failure appearance, test PBF-07 26

20. Pillar post-failure appearance, test PBF-09 27

21. Pillar post-failure appearance, test PBF-10 28

22. Pillar post-failure appearance, test PBF-11 29

23. Pillar post-failure appearance, test PTG-12 30

24. Pillar post-failure appearance, test PBF-13 31

INTRODUCTION

Experimental studies have demonstrated that 'stiff' (cemented rockfill) and 'soft' (cemented tailings) backfill used as confinement of rock pillars can act as passive lateral support (1,2). The backfill confinement provides significant ground stabilization limiting the advance of the failure zones and, by controlling violent pillar failures, alleviates seismic activity in rockburst prone mining excavations.

Extensive large scale experimental work has been conducted to evaluate the interaction of pillar-backfill. The following paper provides the preliminary data from pillar-backfill confinement tests.

ROCK-FILL SPECIMEN PREPARATION AND TESTING

The laboratory experiments performed comprised the following preparation and testing procedures:

1. Rock cores, diameter 136 mm and height/diameter ratio of 2.45 $\pm$0.06, having end parallelism of $\pm$25 μm were prepared. Rock core representing the pillar for the experiments was an andesite with quartz stringers and chlorite-filled fractures obtained from the stress measurement sites at Campbell Red Lake Mine. The rock properties determined were, deformation modulus of 85.0 $\pm$1.3 GPa, Poisson's ratio of 0.20, and a uniaxial compressive strength of 193.0 $\pm$42.0 MPa (3).
2. Aluminum cylinders, ID = 303 mm, OD = 313 mm, height = 380 mm, were prepared and the outer cylinder wall was instrumented using strain gauges spaced at 120^{o} intervals at mid-height. This enabled the monitoring of lateral strains in the cylinder as the pillar-fill specimen was uniaxially compressed.
3. The aluminum cylinder was placed on a plywood plate with holes (diameter ~4 mm) drilled through it to allow drainage of excess water. The rock core was positioned centrally in the cylinder. Tailings were mixed with slag

cement in the ratios of 10, 20, 30, 40 and 50 to 1 tailings to cement in a cement mixer. The mixture was poured into the cylinder and compacted manually.

Tailings properties: Tailings material, currently used by Denison Mine in their Elliot Lake operation, was obtained from the belt filters of a uranium mill after the leaching stage. The unclassified pyritic tailings consisted of a mixture of sand and silt (50% less than 150 μm) with a bulk density of about 65% solid at a moisture content of approximately 40%.

Slag cement properties: Slag cement is obtained as a by-product from a blast furnace (Reiss Lime, Algoma Steel) containing approximately 30% CaO, 30% SiO_2, 9% Al_2O_3 and 15% MgO.

4. The prepared pillar-fill specimen was sealed in a plastic bag and cured for 28 days at room temperature with relative humidity of about 60%.
5. After the curing period, the specimen was removed from the sealed bag and the backfill portion was covered with a 4 mm thick wooden disc with a 136 mm diameter centre hole. This set-up was used to eliminate and/or minimize the possible gap between fill and platen (steel disc), and enable a simultaneous pillar-fill loading.
6. The composite pillar-fill specimen, covered with a steel disc (diameter 300 mm, thickness 20 mm), was uniaxially loaded to pillar failure. An 18 MN closed-loop electrohydraulic 'soft' compression testing machine was used, maintaining a constant loading rate of 1.8 KN/sec. The total load, axial displacement, using 3 displacement transducers (LVDT) spaced at 120^{o}, and the lateral strain from the strain gauges on the test cylinder were monitored. All analog signals were converted for digital acquisition by an A/D converter. A PDP-11 at a sampling rate of 2 samples/sec was used for data acquisition. In addition, to control the testing process, the load-deformation was recorded on a XY recorder. The testing configuration is demonstrated in Figure 1. Figure 2 shows a photograph of a prepared

pillar-backfill specimen in the aluminum cylinder. The 'soft' compression testing machine used for the testing purpose was not capable to control and continue loading at post-peak loading phase. By loading impact at pillar peak strength, the hydraulic system of the press would automatically shut down interrupting the loading process. Therefore, the pillar-backfill specimen was reloaded at the same set-up and loading rate to obtain complete load-deformation curves.

7. The selected testing configuration, i.e., pillar-backfill specimens confined in a 303 mm diameter cylinder, simulated an equivalent extraction ratio of about 75% for a room-and-pillar mining operation with a tabular orebody.
8. In all test specimens, the post-failure appearance of the pillar was examined by removing the consolidated fill from the cylinder.

PRELIMINARY RESULTS

Twelve pillar-backfill confinement tests and 1 confined backfill test were conducted. A summary of the testing program is given in Table 1. The load-deformation curves obtained from the pillar-backfill confinement tests are plotted in Figure 2. Figure 3 summarizes the results of compression characteristics of the confined pillar-backfill specimens. The relationship between vertical stress on pillar-backfill and lateral stress in backfill is shown in Figure 4. After classifying the data, load-deformation for each set of data with varying tailings/cement ratio was identified and plotted in Figures 5 to 9. The graphs also show the post-failure compression (reloaded test specimens) from pillar-backfill confinement tests. Load and displacement from all compression tests have been corrected to adjust for platen tilting at the initial loading phase. From the evaluation of complete load-deformation behaviour of confined rock pillars two failure types were identified as stable and unstable post-failure.

Figure 10 shows the relationship between the residual strength and the tailings/cement ratio in the backfill. To identify the compression characteristics of backfill, test BFL-08 with a tailings/cement ratio of 30:1 was performed. The uniaxial compression loading cycles plotted in Figure 11 clearly demonstrate a progressive stiffening of a 'soft' backfill in lateral confinement.

After removal from test cylinders, pillar-backfill specimens were examined for the post-failure appearance. At the pillar-backfill interface no failure surface was observed, and apparently pillar 'barrelling' had not occurred at the post-failure phase. Most pillars revealed a split failure with single or multiple near-vertical fracturing. Failure also occurred as a combination of vertical splitting and tensile fracturing normal to the pillar axis, producing varying degrees of fragmentation. Some pillars failed along single or multiple shear planes. The post-failure appearance of pillars is illustrated in Figures 12 to 23.

DISCUSSION

The parameters which could influence the result of this experiment can be identified as follows:

i) The geomechanical properties of model pillars.

ii) The physical characteristics of the tailings; grain size distribution, mineralogical composition, etc.

iii) Loading rate, and whether the test is being conducted in a soft or stiff compression testing machine. The pillar post-failure characteristics and the magnitude of residual strength are controlled by the stiffness of the testing machine.

iv) The cement content of the backfill; tailings:cement ratio.

v) The degree of saturation of tailings and the possibility of pore pressure build-up.

vi) The degree of compaction and consolidation of the top portion (10-30 mm) of the backfill.

vii) The contribution of the recorded cumulative strain due to compaction of the wooden disc.

viii) The magnitude of confinement due to compaction of backfill.

Ideally speaking, the influence of each parameter has to be investigated under controlled conditions, and in considering the minimum number of specimens required to arrive at a statistically determined value, a large number of tests would have been required.

In order to obtain a quick set of data within a reasonable time limit, it was decided to test the minimum number of specimens, keeping, as far as possible, some of the above parameters as constants. Out of the eight parameters cited, with the exception of (i) and (ii), which are fixed, the others could be variable.

It is assumed that the rock is homogeneous and the grain size distribution of backfill is uniform. The tailings:cement ratio is the variable throughout the tests, and no attempt at pore pressure measurements were made.

From the examination of the combined load-displacement graphs shown in Figure 2, and the results summarized in Table 1, the following deductions can be made:

1. The model pillar specimens are identical; however, the peak stress recorded has a variation of about 40 MPa. This variation and/or scatter in peak stress sustained by the pillars is attributed to the degree of confinement offered by the backfill.
2. The ratio of residual strength/peak strength is independent from the magnitudes of peak strength.
3. The residual strength/peak strength ratio and residual strength increases with the degree of confinement, as expected. The instrumentation of the

aluminum cylinder provides the lateral stresses sustained by the pillar-backfill specimen. By implementation of the elastic theory a value for the degree of confinement using the deduced Poisson's ratio could be calculated. However, this value should ideally be measured by strain gauging the rock pillars and measurement of ϵ_L and ϵ_V for the duration of the test.

4. The third significant parameter is the presence of a gap between the pillar-backfill specimen and the loading platen, which, in conjunction with the wooden disc, would introduce erroneous values of stress into the calculation. The standardization of the initial void ratio of the specimen prior to testing, by compacting them at a standard load at a specified time, would significantly reduce this error.

In conclusion the preliminary results from this series of tests provide meaningful data with regard to the effect of soft backfill in controlling the pillar failure characteristics. However, additional tests are needed to conclusively establish a mathematical relationship for pillar-backfill interaction.

ACKNOWLEDGEMENT

The cooperation of Denison Mines Ltd., Elliot Lake, for providing the tailings material is appreciated.

REFERENCES

1. Blight, G.E. and Clarke, I.F., "Design and properties of stiff fill for lateral support"; Proc. Int. Symp. Mining and Backfill, Lulea, Sweden, June 1983.

2. Swan, G. and Beard, M., "Fill-induced post-peak pillar stability"; Proc. Innovations in Mining Backfill Technology, Montreal, October 1989.

3. Arjang, B., "Review and evaluation of ground stresses at Campbell Red Lake Mine, Ontario"; Division Report MRL 87-108(TR), CANMET, Energy, Mines and Resources Canada, 1987.

Table 1 - Summary of confined pillar-backfill testing.

Test Code (1)	Tailings/ Cement Ratio	Rock Core 'Pillar' H/D Ratio (3)	Peak(P) Strength (MPa)	Residual(R) Strength (MPa)	R/P Ratio	Failure Mode	Post-Failure Appearance (2)	Remarks
PBF-01	10:1	2.60	223.0	146.0	0.65	Non-violent	SF,FG	BF, consolidated
PBF-02	10:1	2.48	180.0	170.0	0.70	Non-violent	SF,FG	BF, consolidated
PBF-03	10:1	2.40	263.0	145.0	0.56	Semi-violent	SP	BF, consolidated
PBF-04	20:1	2.53	175.0	110.0	0.63	Semi-violent	SF,FG	BF, pt. unconsol.
PBF-05	20:1	2.48	228.6	103.0	0.45	Semi-violent	SF,FG	BF, pt. unconsol.
PBF-06	30:1	2.43	192.0	105.0	0.55	Non-violent	SF,FG	BF, consolidated
PBF-07	30:1	2.43	120.3	74.0	0.61	Non-violent	SF,FG	BF, consolidated
PBF-11	30:1	2.48	195.4	98.0	0.50	Non-violent	SF,FG	BF, consolidated
PBF-09	40:1	2.44	195.5	68.0	0.35	Semi-violent	MSP,FG	BF, weakly cemented
PBF-10	40:1	2.40	213.8	62.0	0.29	Semi-violent	SF,FG	BF, weakly cemented
PBF-13	50:1	2.45	203.0	47.0	0.23	Violent	SF,HFG	BF, uncemented
PTG-12	-	2.38	124.0	31.0	0.25	Violent	SF,HFG	Tailings only
BFL-08	10:1	-	-	-	-	-	-	Confined BF only

Notes: (1) Test code: PBF - Pillar-backfill; PTG - Pillar-tailings; BFL, BF - Backfill.
(2) Post-failure appearance: SF - Split failed and tensile fracturing; FG - Fragmented; HFG - Highly fragmented and crushed; SP - Single shear plane; MSP - Multiple shear planes.
(3) Core diameter 136 mm, height 277-354 mm.

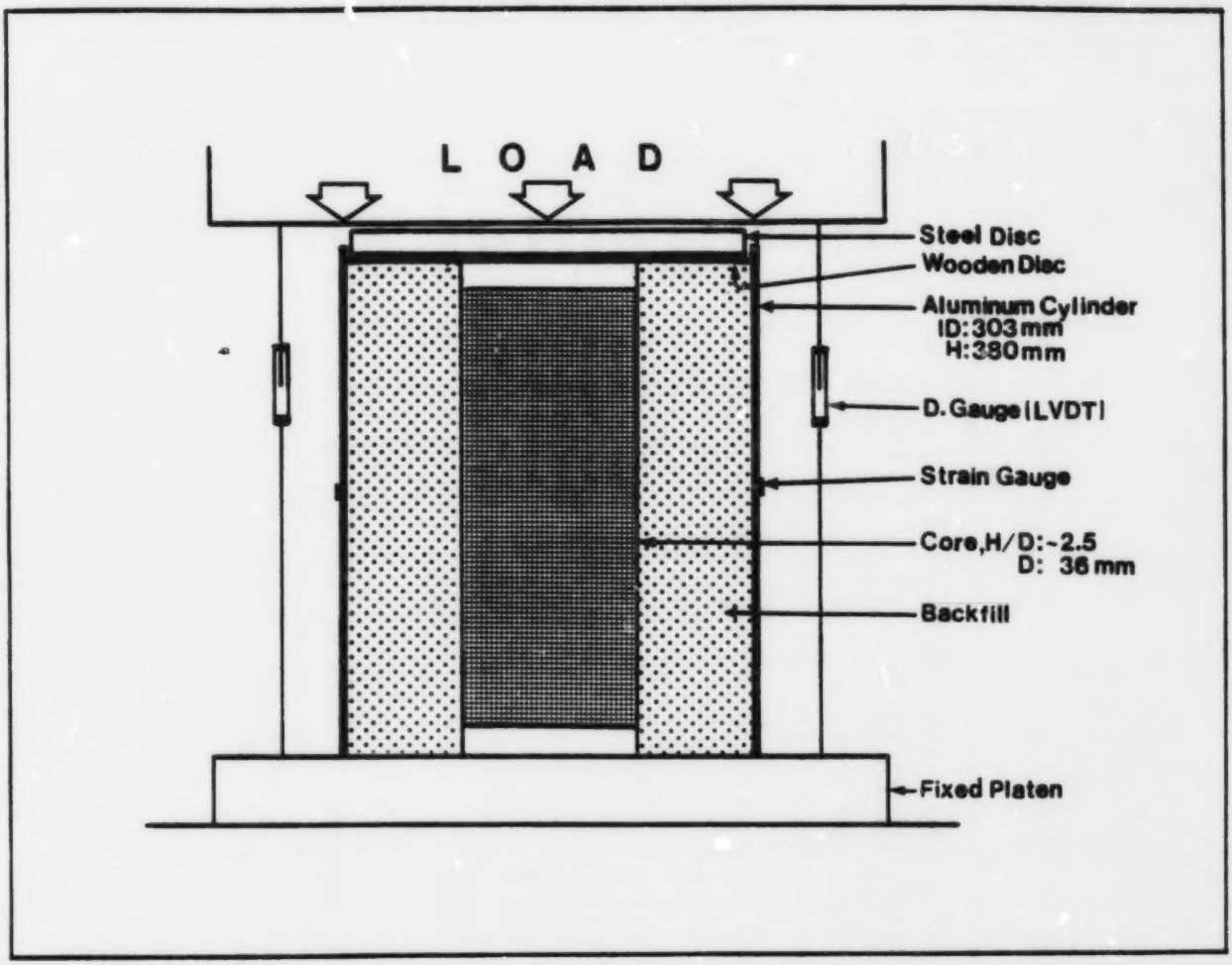

Fig. 1 - Sectional diagram of testing configuration.

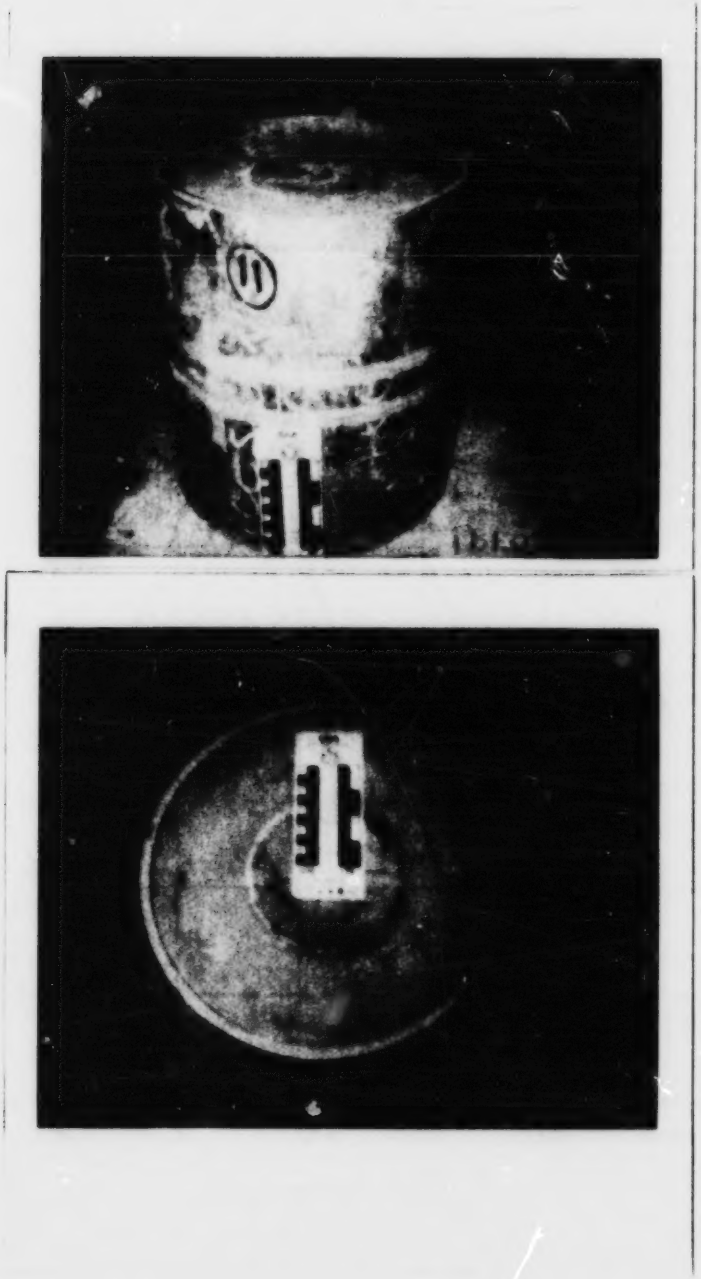

Fig. 2 - Photographs showing the pillar-backfill test specimen in the aluminum cylinder.

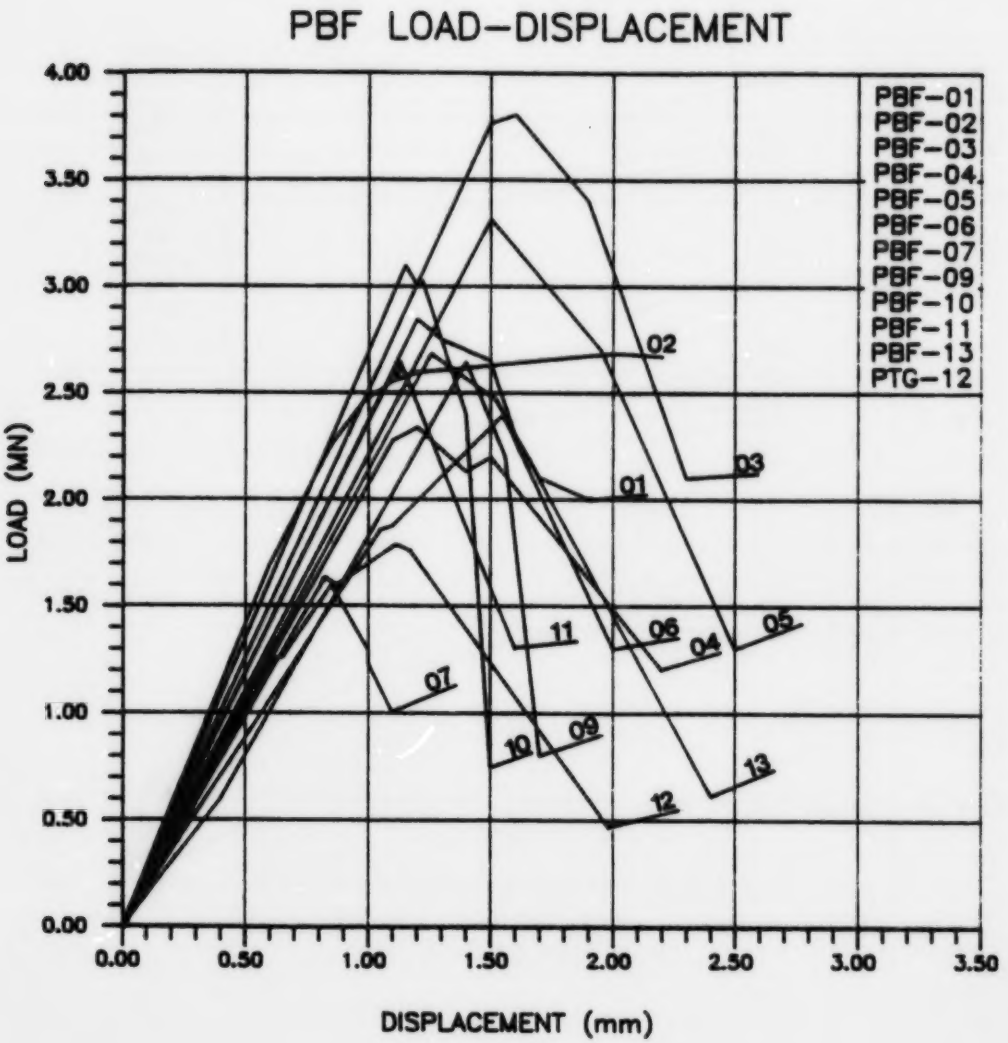

Fig. 3 - Load-displacement curves from pillar-backfill confinement tests.

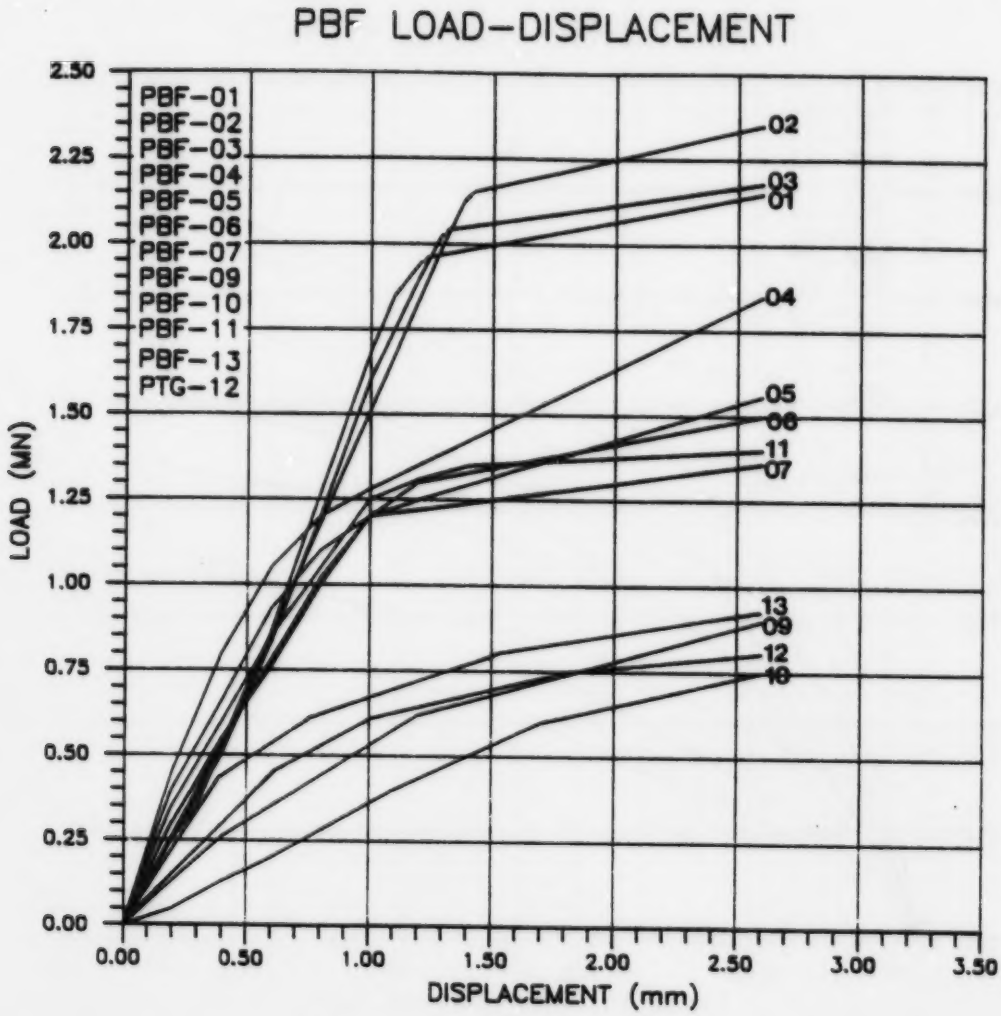

Fig. 4 - Load-displacement curves from post-failure compression on confined pillar-backfill specimens.

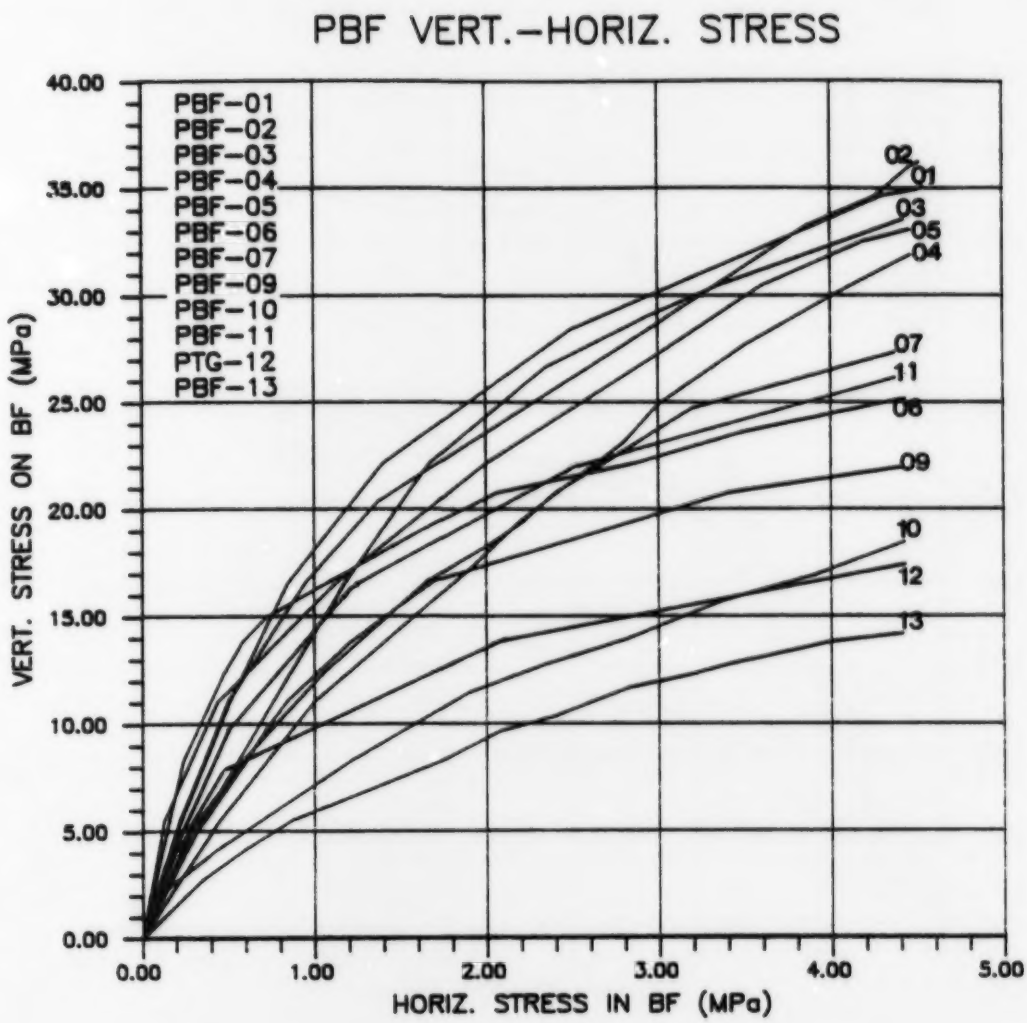

Fig. 5 - Relationship between vertical stress on the confined pillar-backfill and lateral stress in backfill.

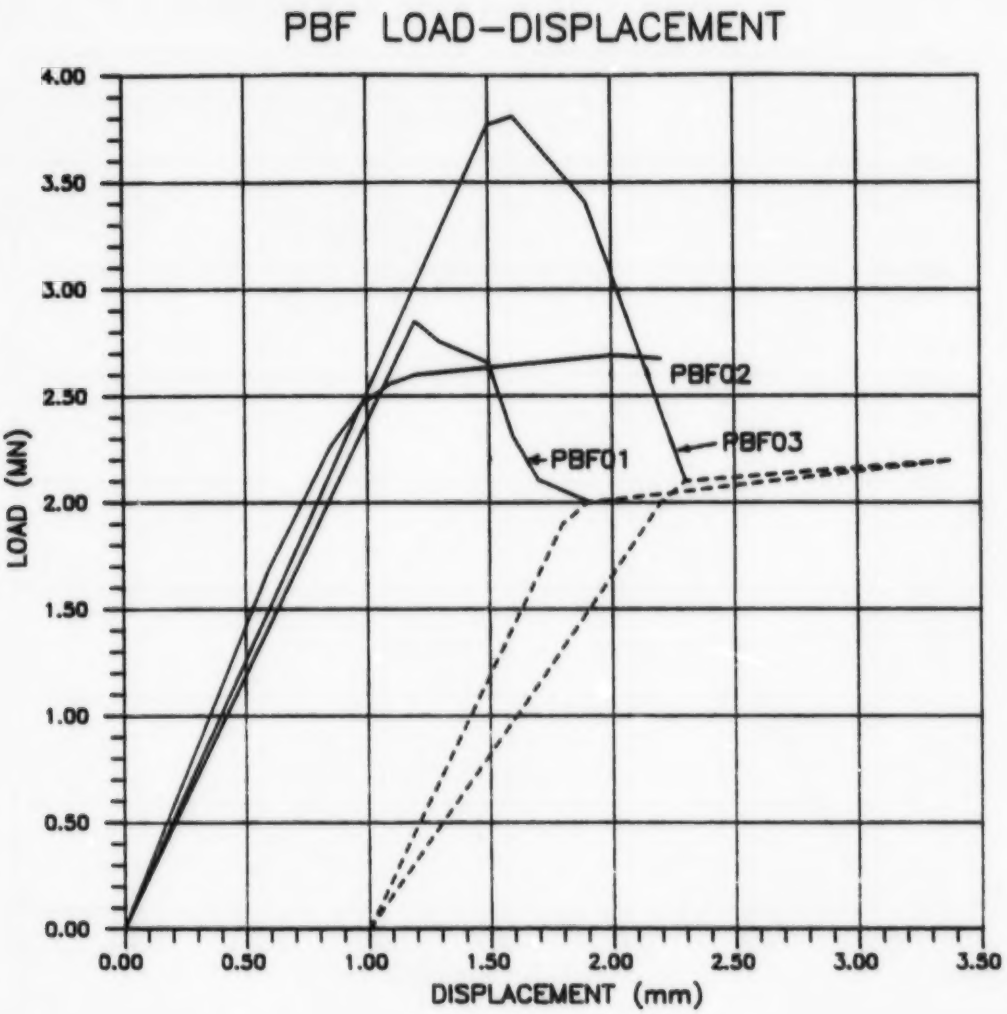

Fig. 6 - Combined graphs of load-displacement and post-failure compression (dashed curves) from pillar-backfill confinement; backfill ratio 10:1, test No. PBF-01, PBF-02 and PBF-03.

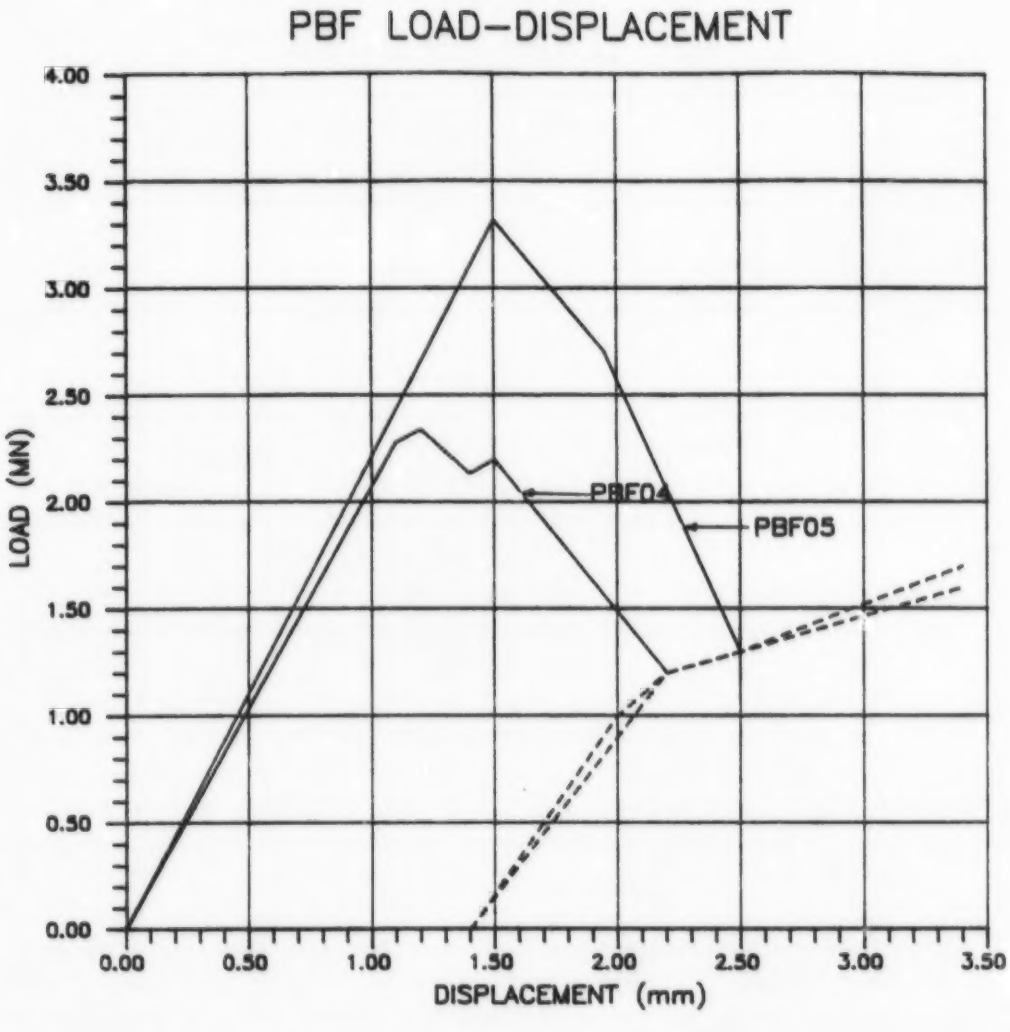

Fig. 7 - Combined graphs of load-displacement and post-failure compression (dashed curves) from pillar-backfill confinement; backfill ratio 20:1, test No. PBF-04 and PBF-05.

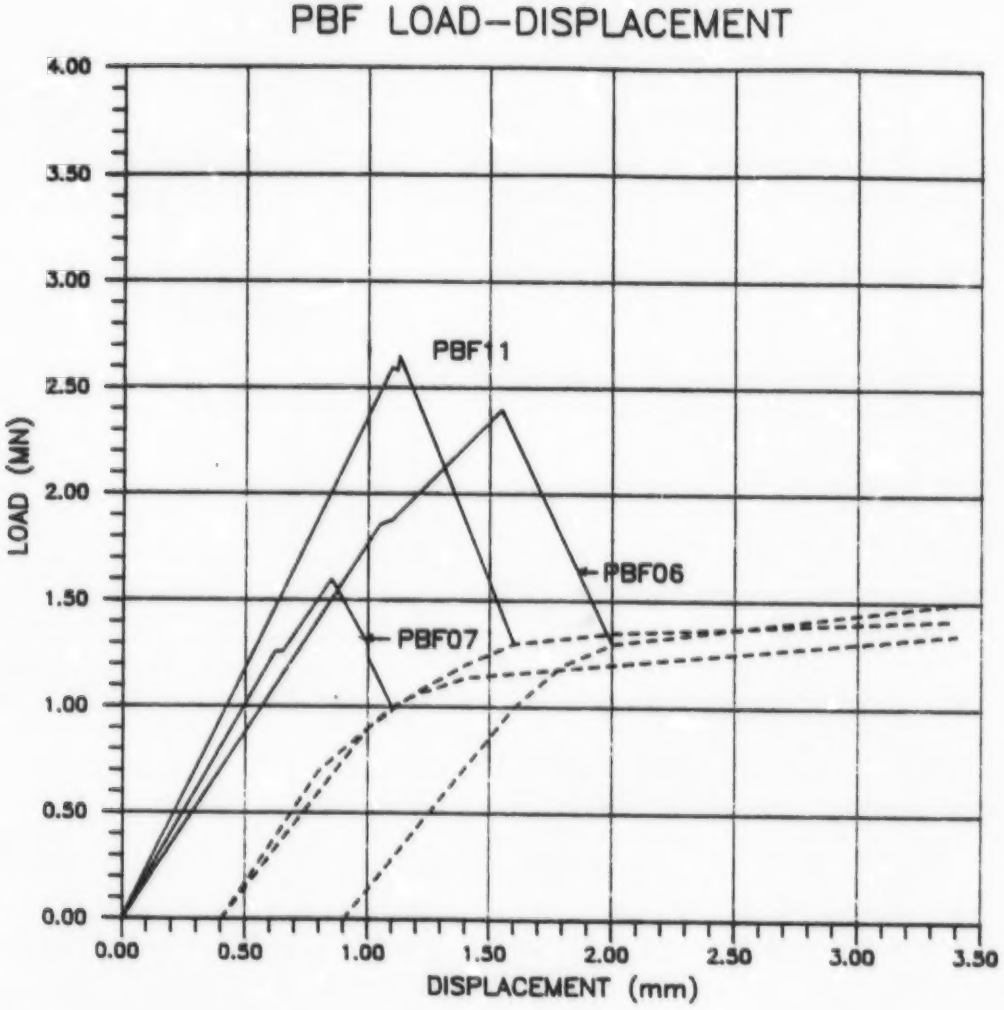

Fig. 8 - Combined graphs of load-displacement and post-failure compression (dashed curves) from pillar-backfill confinement; backfill ratio 30:1, test No. PBF-06, PBF-07 and PBF-11.

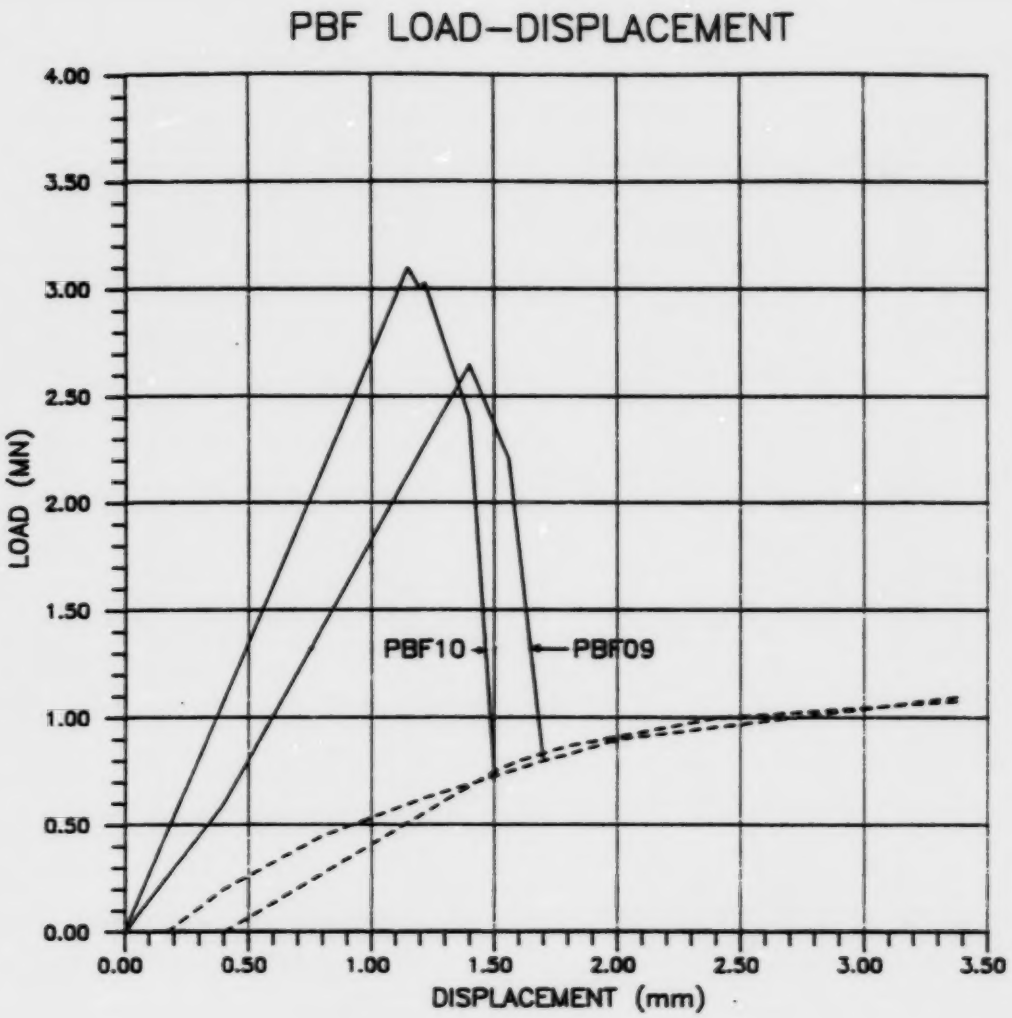

Fig. 9 - Combined graphs of load-displacement and post-failure compression (dashed curves) from pillar-backfill confinement; backfill ratio 40:1, test No. PBF-09 and PBF-10.

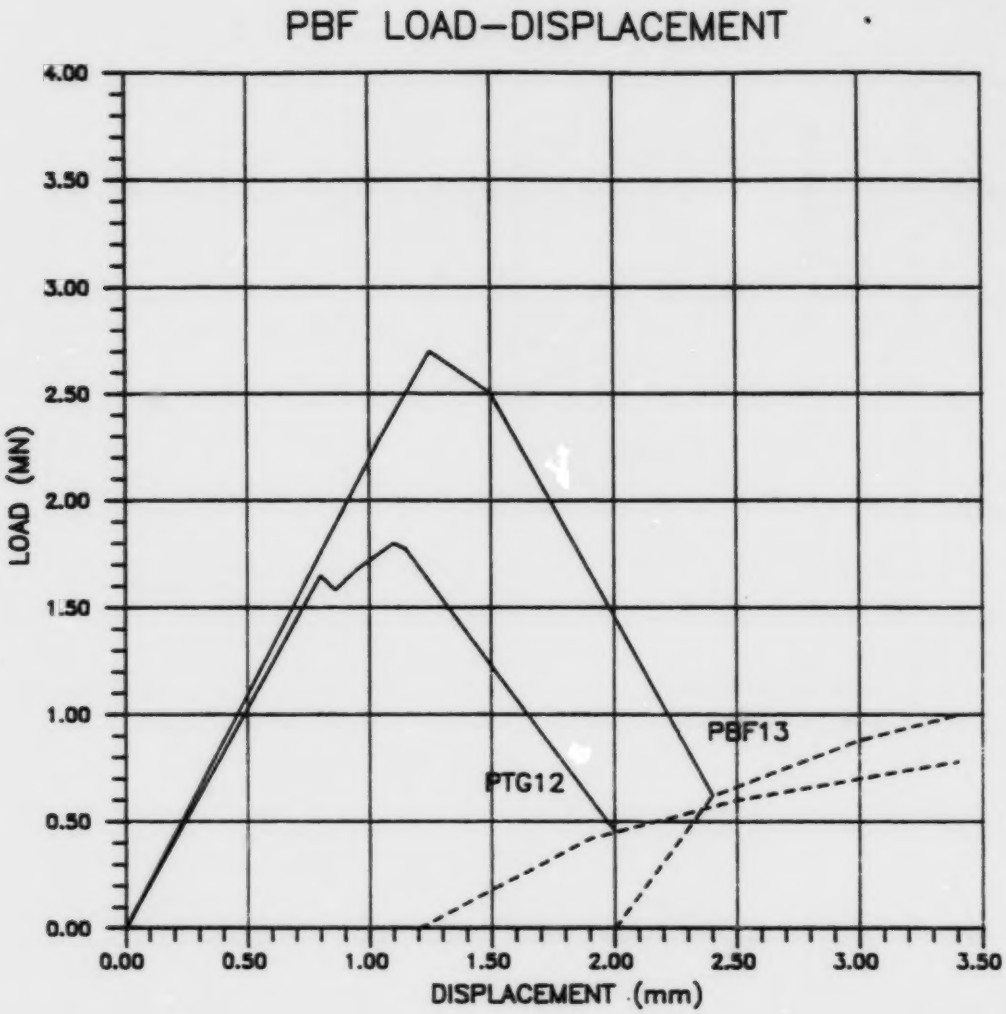

Fig. 10 - Combined graphs of load-displacement and post-failure compression (dashed curves) from pillar-backfill confinement; backfill ratio 50:1, test No. PBF-13 and PTG-12 pillar-tailings.

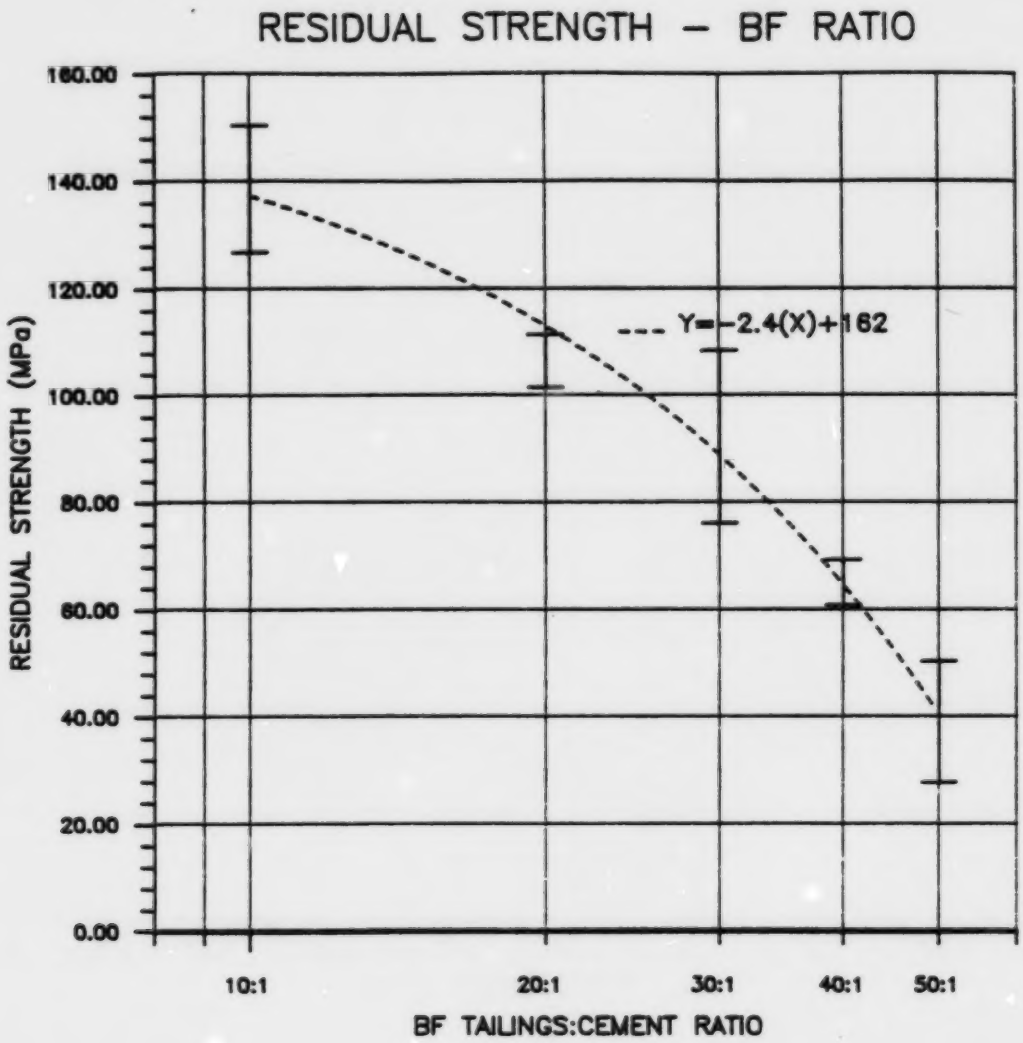

Fig. 11 - Relationship between the residual strength and the backfill tailings:cement ratio.

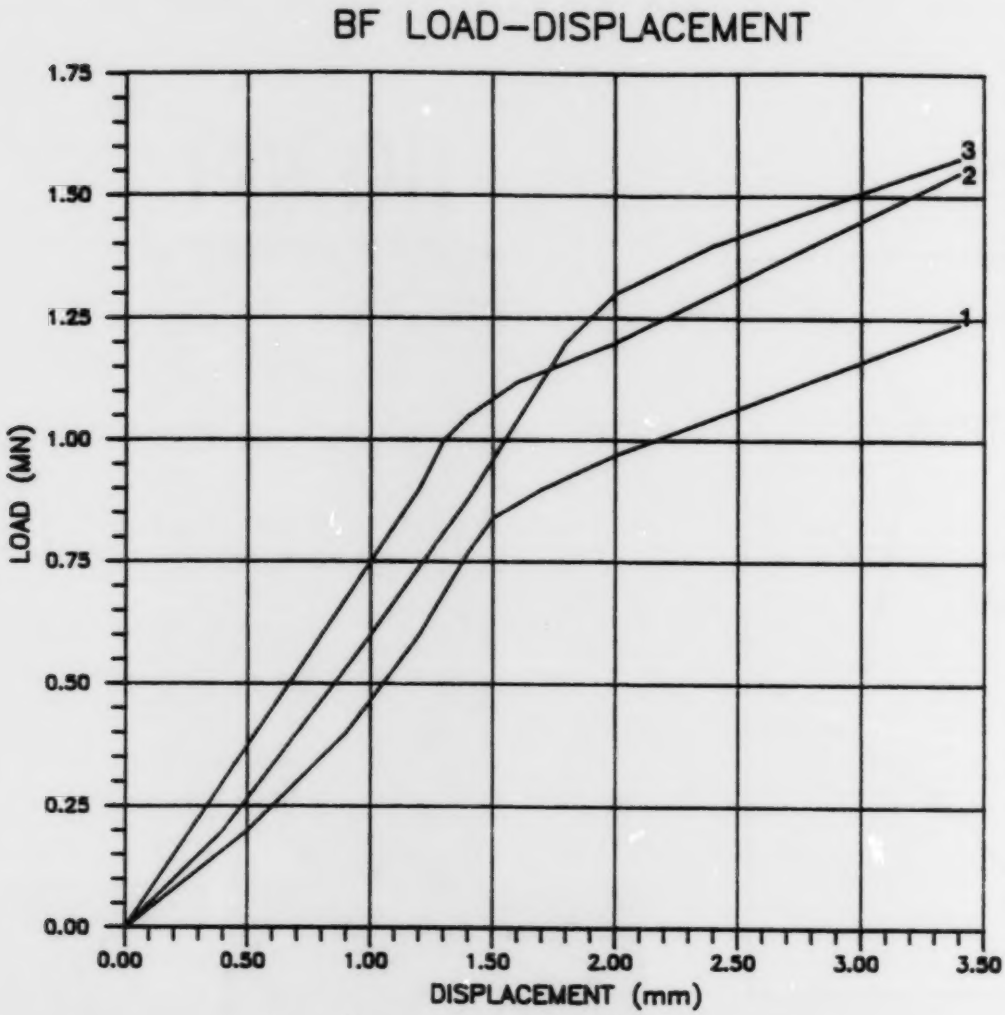

Fig. 12 - Load-displacement curves from uniaxial compression cycles on a confined backfill (30:1).

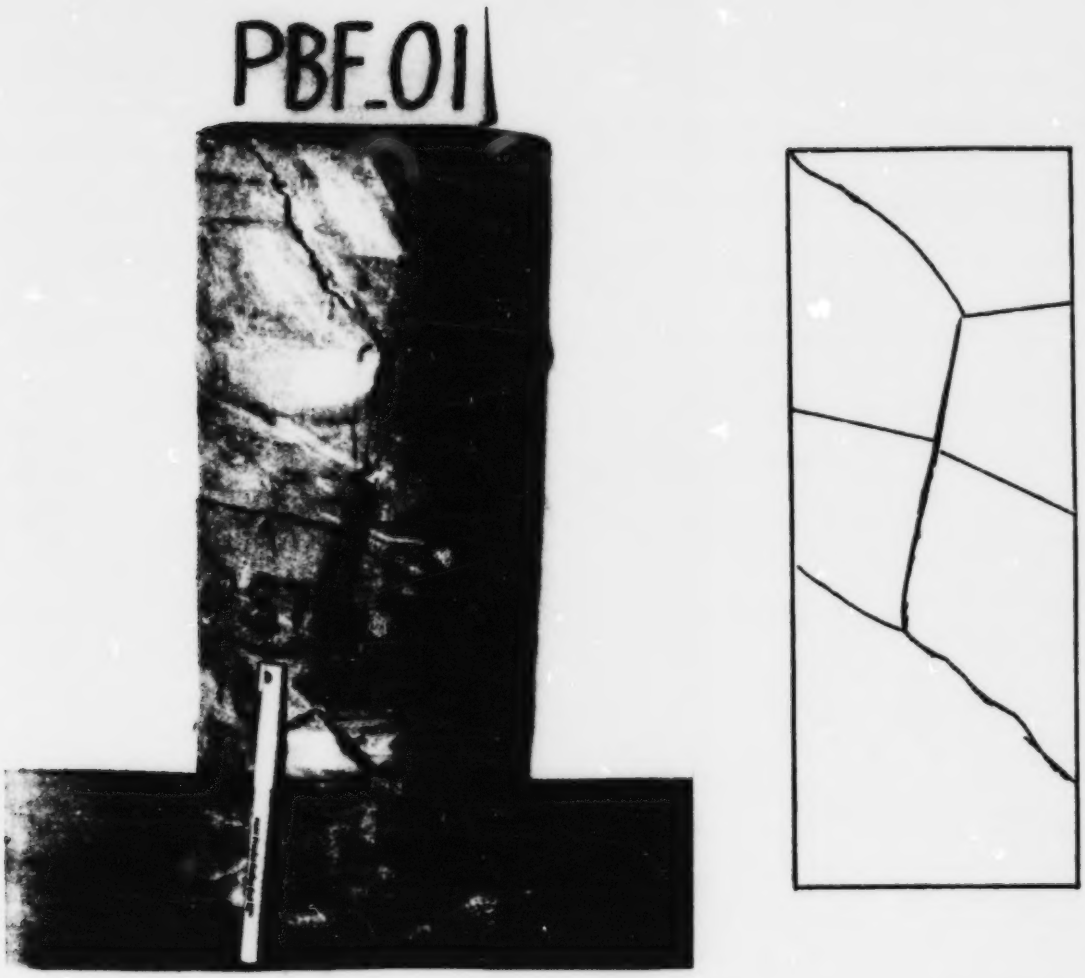

Fig. 13 - Pillar post-failure appearance, test PBF-01.

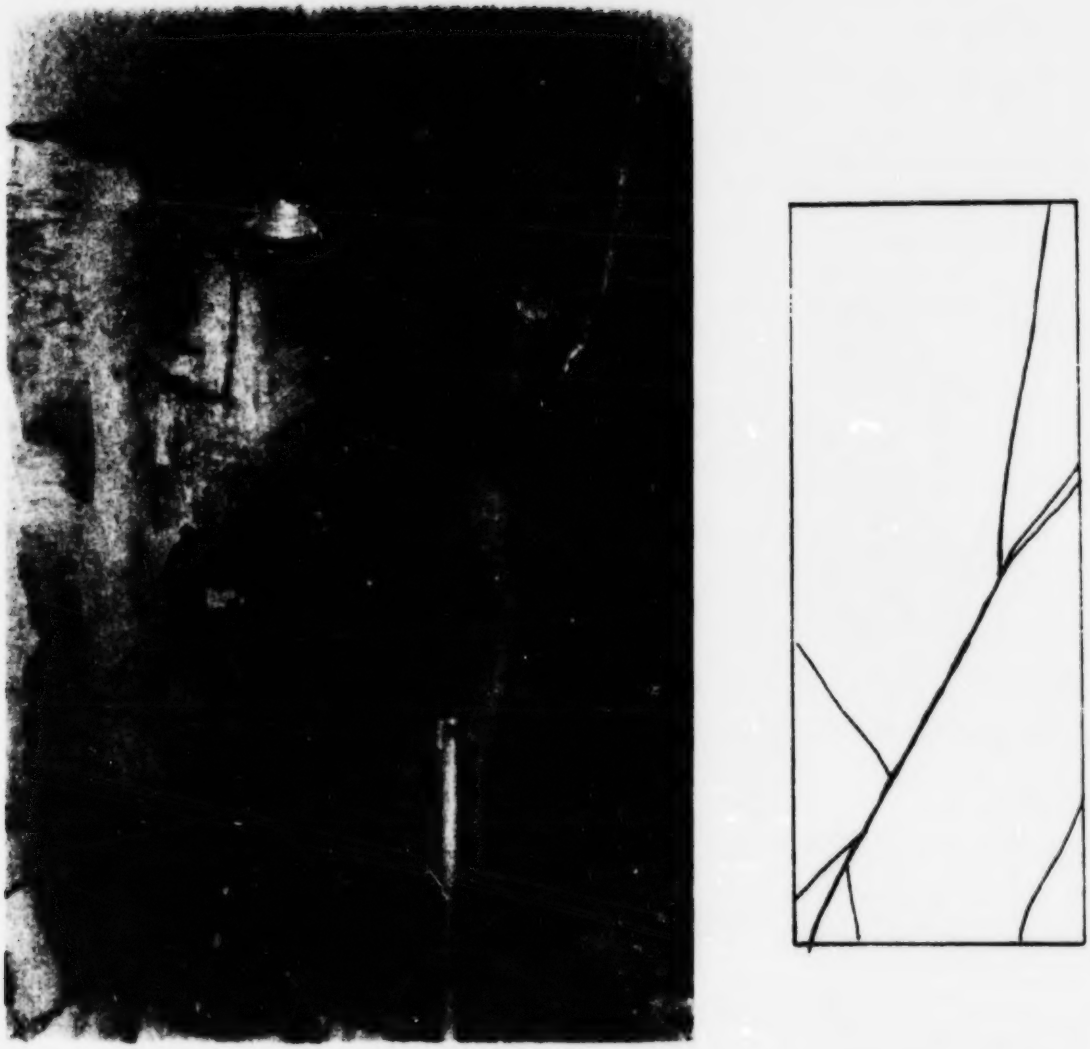

Fig. 14 - Pillar post-failure appearance, test PBF-02.

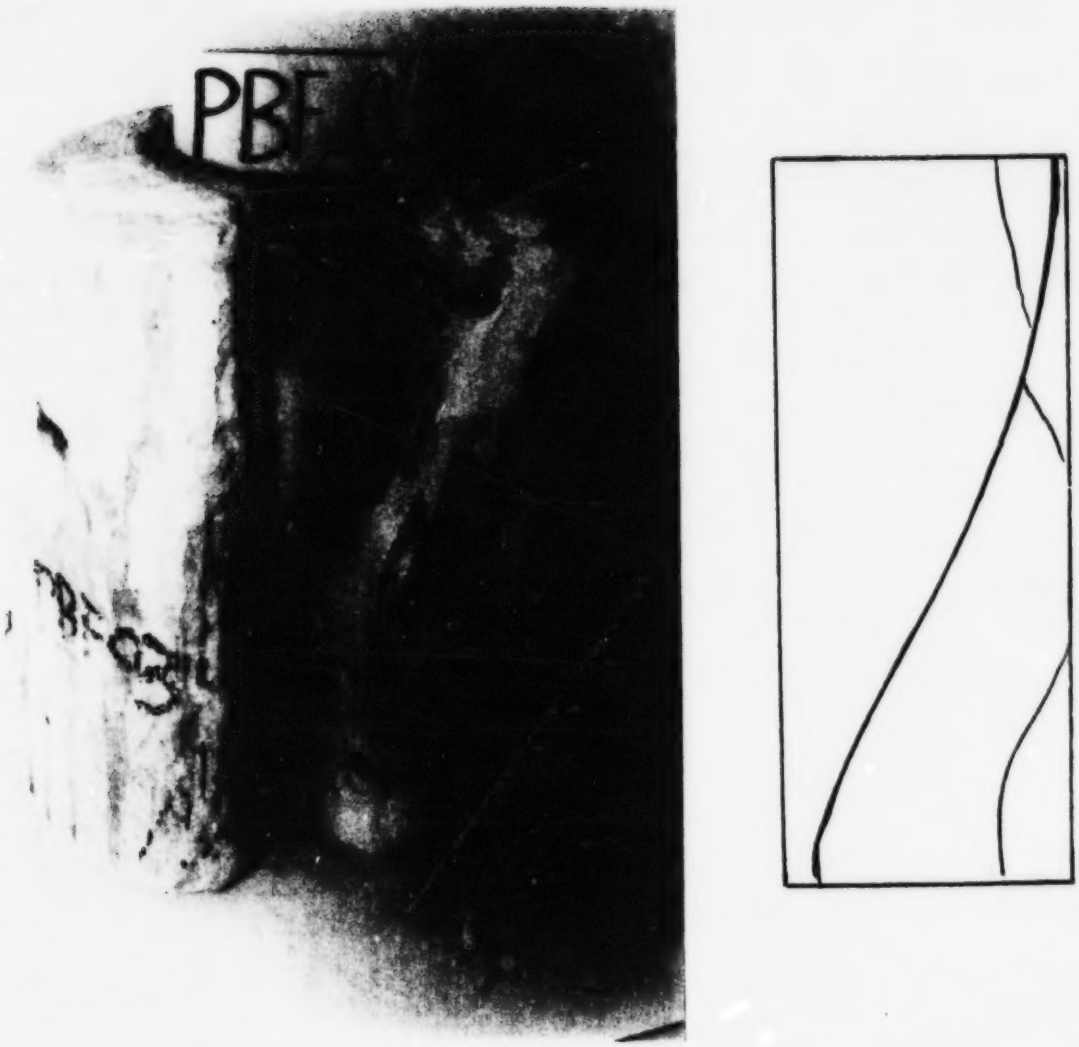

Fig. 15 - Pillar post-failure appearance, test PBF-03.

Fig. 16 - Pillar post-failure appearance, test PBF-04.

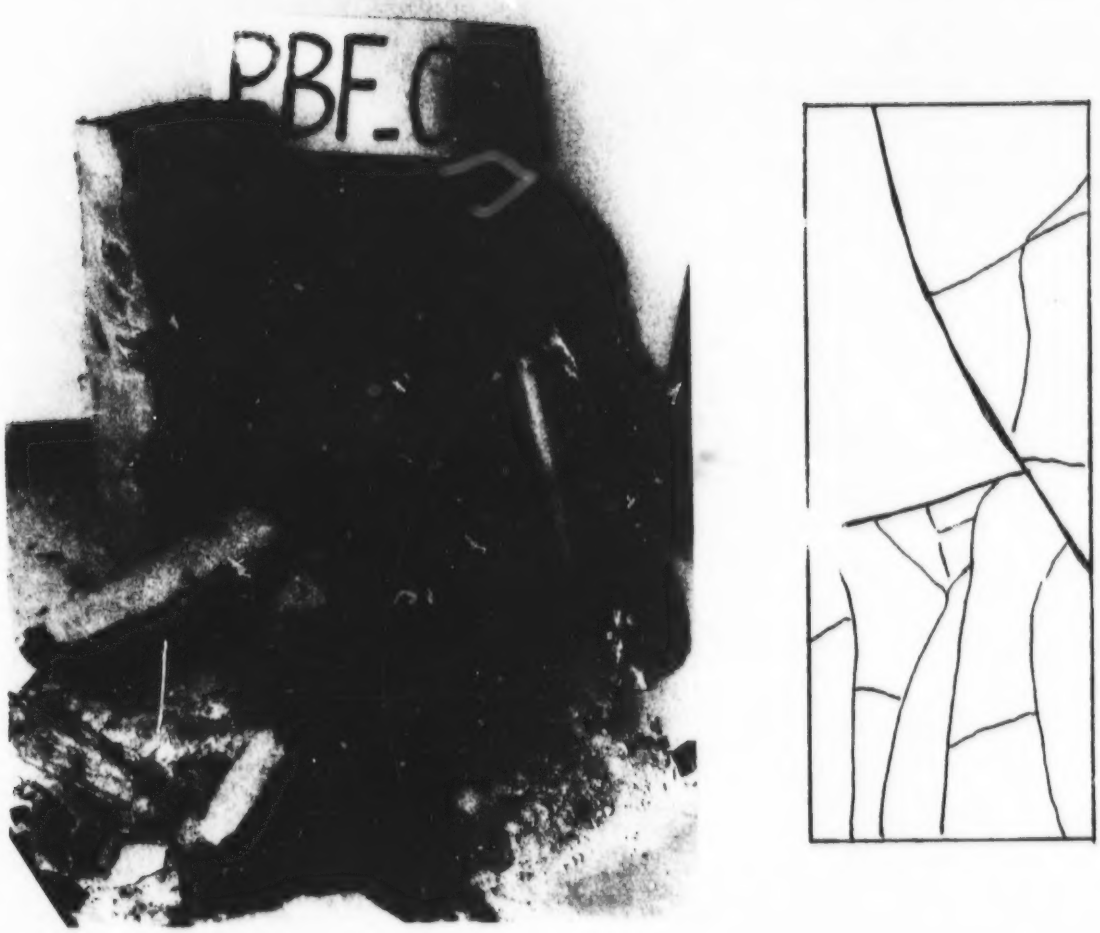

Fig. 17 - Pillar post-failure appearance, test PBF-05.

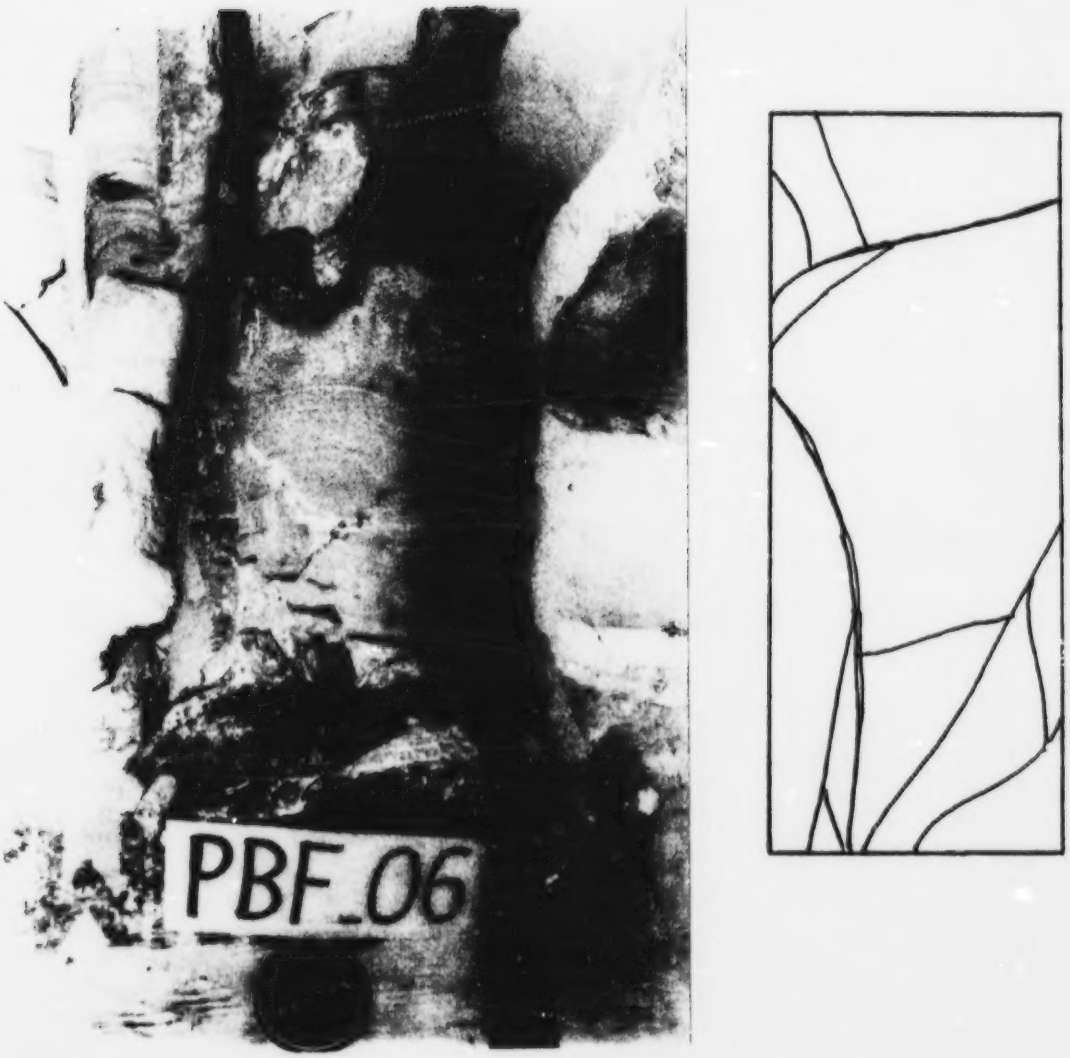

Fig. 18 - Pillar post-failure appearance, test PBF-06.

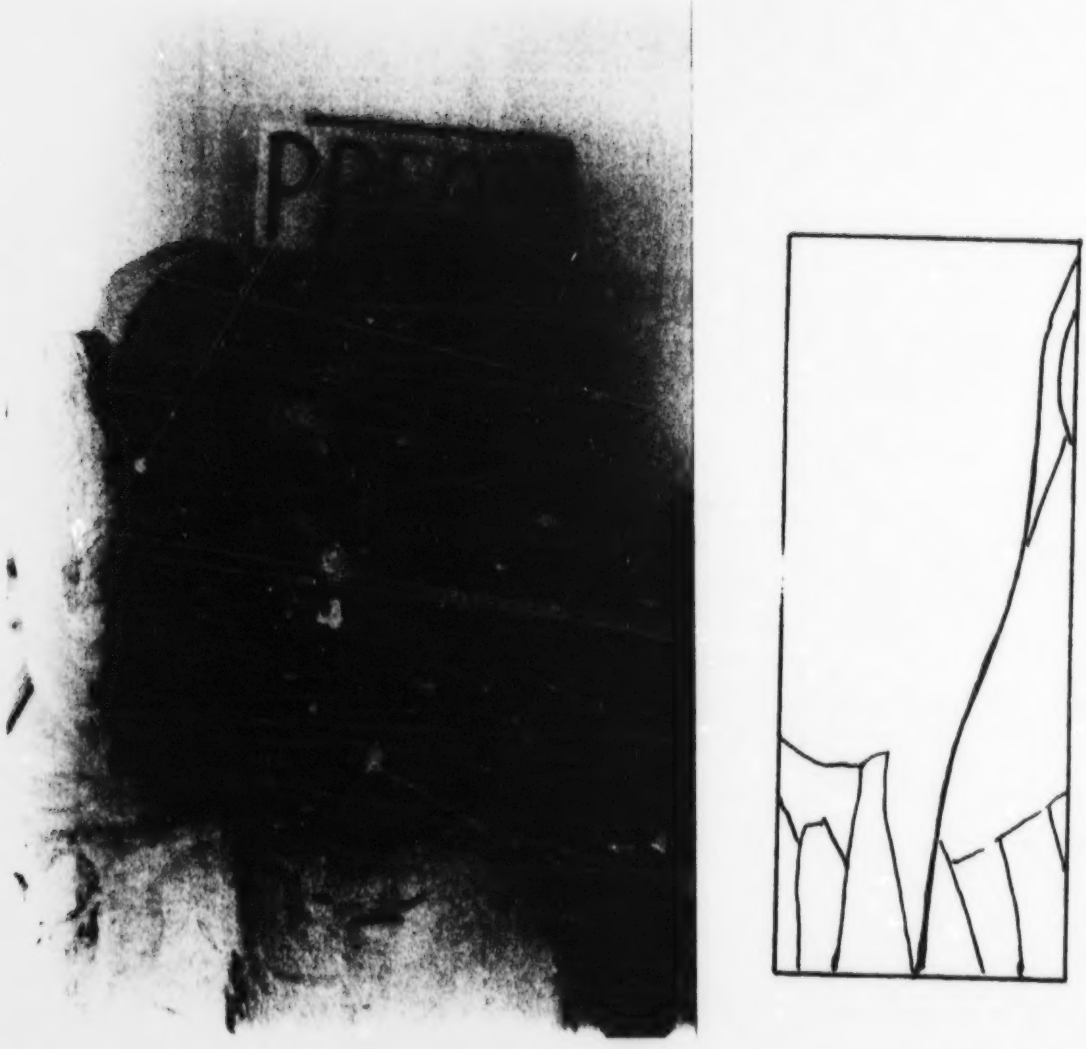

Fig. 19 - Pillar post-failure appearance, test PBF-07.

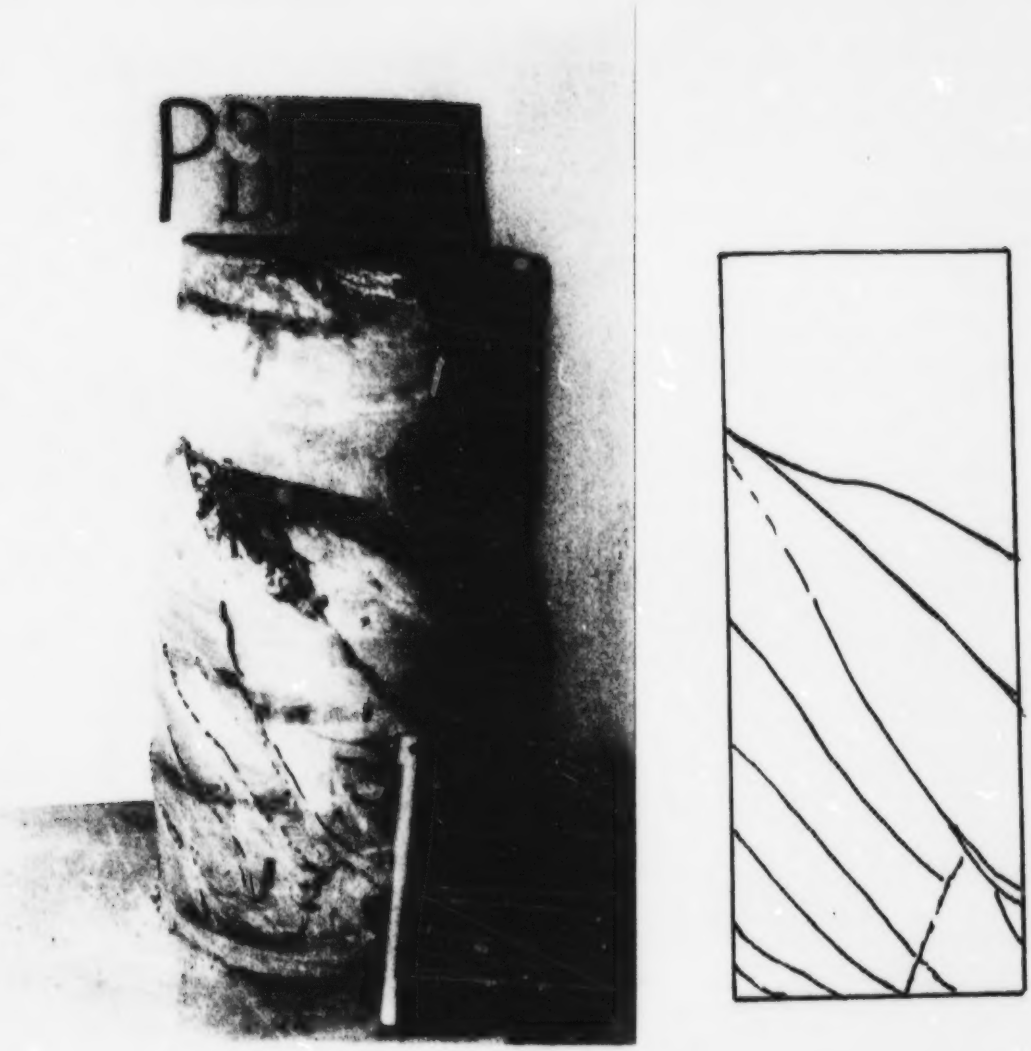

Fig. 20 - Pillar post-failure appearance, test PBF-09.

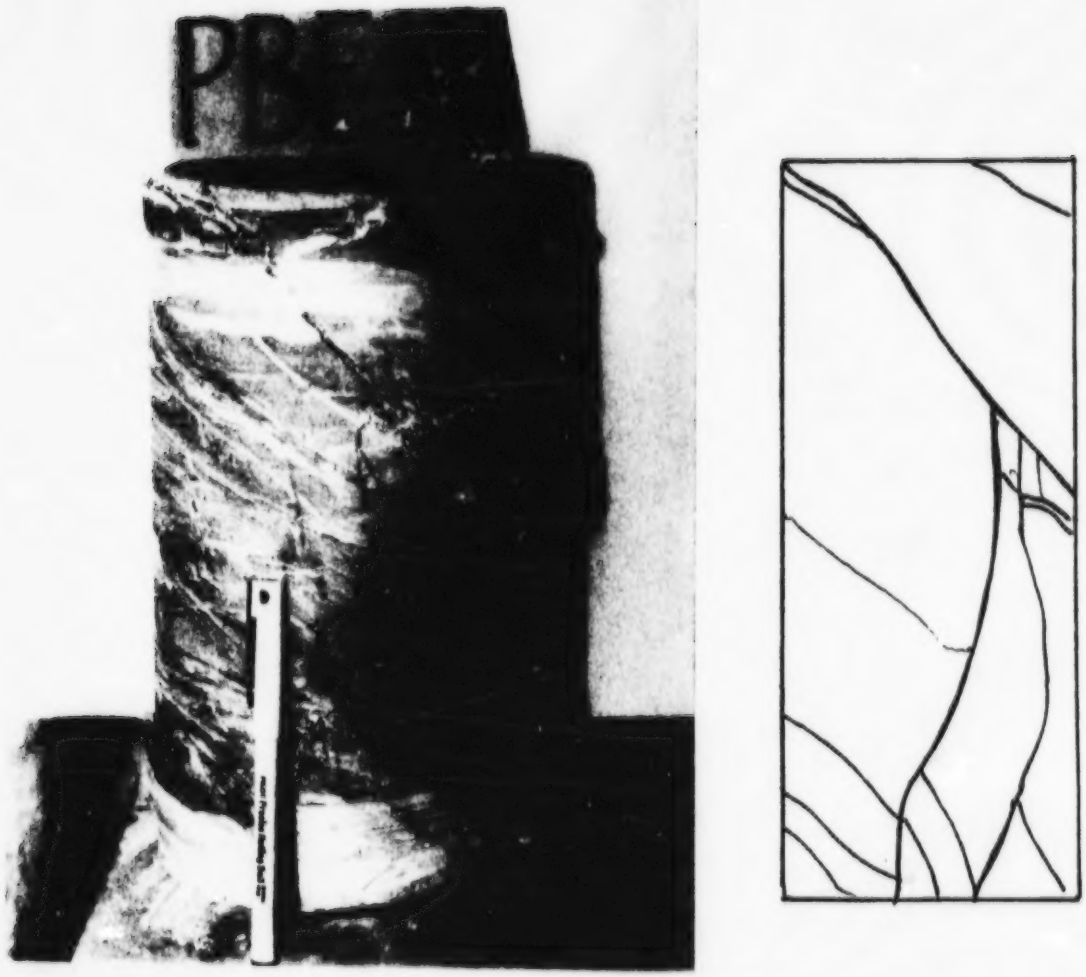

Fig. 21 - Pillar post-failure appearance, test PBF-10.

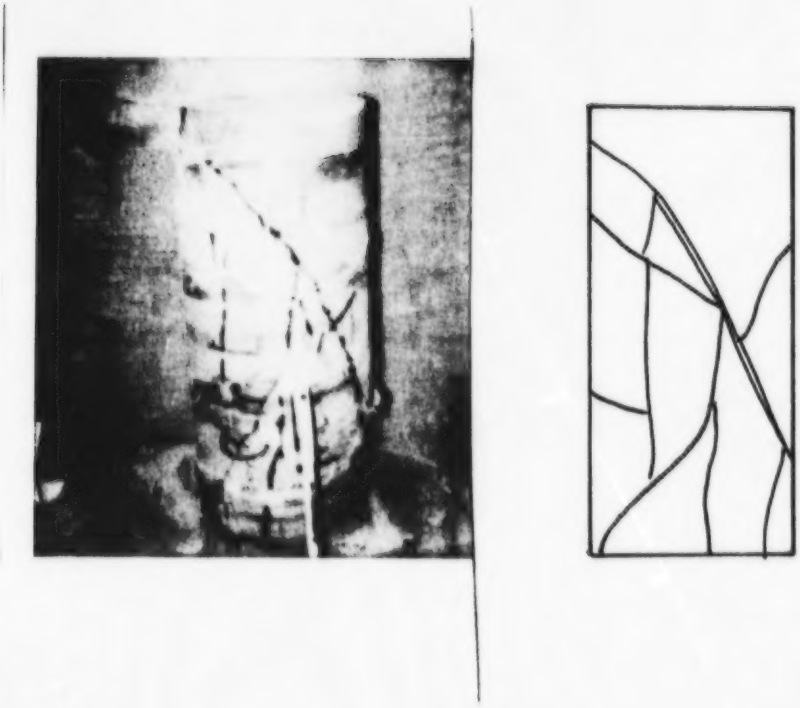

Fig. 22 - Pillar post-failure appearance, test PBF-11.

Fig. 23 - Pillar post-failure appearance, test PTG-12.

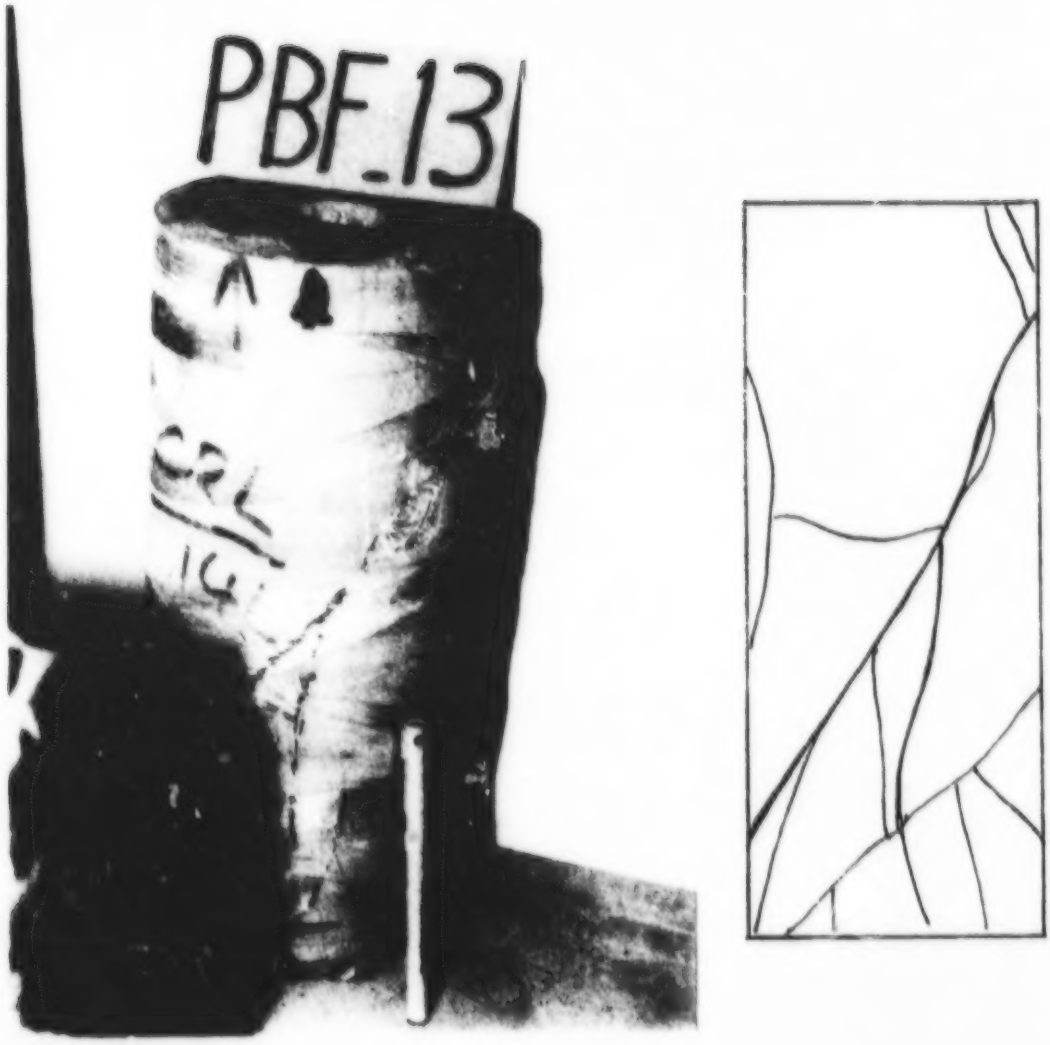

Fig. 24 - Pillar post-failure appearance, test PBF-13.